Journal of Solid State Chemistry 182 (2009) 1889–1898

Contents lists available at ScienceDirect

Journal of Solid State Chemistry

journal homepage: www.elsevier.com/locate/jssc

The tunable coordination architectures of a flexible multicarboxylate *N*-(4-carboxyphenyl)iminodiacetic acid via different metal ions, pH values and auxiliary ligand

Xiaochuan Chai [a], Hanhui Zhang [a,b,*], Shuai Zhang [a], Yanning Cao [a], Yiping Chen [a]

[a] Department of Chemistry, Fuzhou University, Fuzhou, Fujian 350108, PR China
[b] State Key Laboratory of Structural Chemistry, Fujian Institute of Research on the Structure of Matter, The Chinese Academy of Sciences, Fuzhou, Fujian 350002, PR China

ARTICLE INFO

Article history:
Received 13 January 2009
Received in revised form
29 April 2009
Accepted 3 May 2009
Available online 10 May 2009

Keywords:
N-(4-carboxyphenyl)iminodiacetic acid
Coordination architectures
2D correlation analysis of FTIR
Fluorescent emission

ABSTRACT

$\{[Pb_3(CPIDA)_2(H_2O)_3]\cdot H_2O\}_n$ **1**, $\{[Cd_3(CPIDA)_2(H_2O)_4]\cdot 5H_2O\}_n$ **2**, $[Cd(HCPIDA)(bpy)(H_2O)]_n$ **3** (bpy = 4,4′-bipyridine) and $\{[Co_3(CPIDA)_2(bpy)_3(H_2O)_4]\cdot 2H_2O\}_n$ **4** were synthesized with *N*-(4-carboxyphenyl) iminodiacetic acid (H_3CPIDA). In **1**, the $CPIDA^{3-}$ ligands adopt chelating and bridging modes with Pb(II) to possess a 3D porous framework. In 2D-layer **2**, the $CPIDA^{3-}$ ligands display a simple bridging mode with Cd(II). The 2D layers have parallelogram-shaped channels along *a* axis. With bpy ligands, the $HCPIDA^{2-}$ ligands in **3** show more abundant modes, but **3** still displays a 2D sheet on *bc* plane for the unidentate bpy molecules. However, in 3D-framework **4**, the bpy ligands adopt bridging bidentate at a higher pH value and the $CPIDA^{3-}$ ligands show bis-bidentate modes with Co(II). Additionally, 2D correlation analysis of FTIR was introduced to ascertain the characteristic adsorptions location of the carboxylate groups with different coordination modes in **4** with thermal and magnetic perturbation. Compounds **1**, **2** and **4** exhibit the fluorescent emissions at room temperature.

1. Introduction

The metal-organic frameworks (MOFs) have received intense interest, mostly motivated by their intriguing variety of architectures and potential properties in applications: gas storage, catalysis, magnetism, nonlinear optics, etc. [1–7]. Yaghi and coworkers have demonstrated that MOFs can be designed and constructed through control of the architectures and functionalization of organic linkers [8–12]. Recently, multicarboxylate ligands are often selected as multifunctional organic linkers because of the abundant coordination modes such as terminal unidentate, chelating, bridging bidentate and bridging tridentate [13], and also because of the ability to act as hydrogen bond acceptors and atoms to assemble supramolecular structures [14]. For example, benzene dicarboxylate and benzene tricarboxylate have been investigated widely for the design and synthesis of frameworks with diverse structures [15–17].

However, the coordination polymers constructed from the flexible multicarboxylate ligand *N*-(4-carboxyphenyl)iminodiacetic acid (H_3CPIDA) were rarely reported [18,19]. Besides the considerations mentioned above about multicarboxylate ligands, H_3CPIDA has its own remarkable features. (a) It holds multiple coordination sites with multipotential groups, i.e., the rigid carboxylate group, the nitrogen atom and two carboxylate groups of the iminodiacetate part, which can afford more abundant types of coordination architectures together. (b) Two carboxylate groups from the flexible iminodiacetate part, which contains the flexible $-CH_2-$ groups, are more sensitive toward metal atoms. They can freely twist to meet the requirements of the coordination geometries of metal atoms, and may induce metal clusters and link these clusters into an extended framework with various coordination modes. (c) The aromatic rings may provide additional $\pi-\pi$ stacking interactions to form interesting supramolecular frameworks [20]. The coordination modes of H_3CPIDA found in this work are listed in Scheme 1. Except the mode in part (c) [18], the others are first reported.

The carboxylate groups adopting different modes result in the different spectral features of the bands of COO groups. But these features are hardly observed in 1D FTIR spectrum for the overlapped adsorptions. In order to distinguish the characteristic bands of COO from different coordination modes, herein, 2D correlation analysis proposed by Noda [21–24] was applied. Our group has successfully introduced 2D correlation analysis of FTIR with external thermal and magnetic perturbation to the polyoxometalates and MOFs [25–30]. The results indicate that it is not only necessary to recognize the structure, but also provide valuable information of subtle spectral changes induced by thermal and magnetic perturbation.

In this work, fortunately, four novel coordination polymers $\{[Pb_3(CPIDA)_2(H_2O)_3]\cdot H_2O\}_n$ **1**, $\{[Cd_3(CPIDA)_2(H_2O)_4]\cdot 5H_2O\}_n$

* Corresponding author at: Department of Chemistry, Fuzhou University, Fuzhou, Fujian 350108, PR China. Fax: +86 59187893239.
E-mail addresses: zhanghh1840@hotmail.com, hhzhang@fzu.edu.cn (H. Zhang).

0022-4596/$ - see front matter © 2009 Elsevier Inc. All rights reserved.
doi:10.1016/j.jssc.2009.05.007

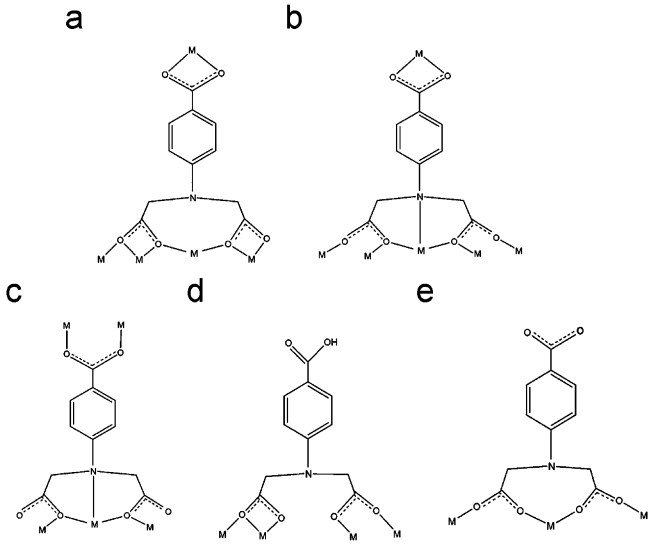

Scheme 1. The coordination modes found in this work: (a) chelating bidentate and chelating/bridging bis-bidentate; (b) chelating bidentate and bridging bis-bidentate (c) bidentate and bridging bis-unidentate; (d) chelating/bridging bidentate and bidentate; (e) bis-bidentate.

2, $[Cd(HCPIDA)(bpy)(H_2O)]_n$ **3** and $\{[Co_3(CPIDA)_2(bpy)_3(H_2O)_4]\cdot 2H_2O\}_n$ **4** were synthesized in the absence or presence of bpy ligands at lower pH values. Employing 2D correlation analysis of FTIR, the carboxylate groups adopting different coordination modes in **4** were detected with thermal and magnetic perturbation. In addition, the fluorescent properties of **1**, **2** and **4** were investigated in detail.

2. Experimental

2.1. General procedures

The ligand H_3CPIDA was prepared according to the literature methods [18,19,31] and other materials were commercially purchased and used without purification. The elemental analyses of C, H, and N were performed with an Elementar Vario EL III elemental analyzer. The powder XRD patterns were recorded on a PANalytical X' pert Pro diffractometer equipped with Cu$K\alpha$ radiation ($\lambda = 1.5406$ Å) at room temperature. Ultraviolet–visible diffuse reflection integral spectra (UV–Vis DRIS) were measured by a Perkin-Elmer Lambda 900 UV–Vis spectrometer with $BaSO_4$ as the reference sample. The IR spectra were recorded with a Perkin-Elmer Spectrum 2000 FT-IR spectrometer in the range of 400–4000 cm^{-1} using the KBr pellet technique. In order to get the 2D correlation FTIR spectra, the thermal intensity variation was taken by a thermal controller from 50 to 120 °C at intervals of 10 °C. On the other hand, the magnetic intensity variation was controlled by a home-made magnetic intensity controller from 2 to 20 mT at intervals of 2 mT. By way of parenthesis introducing, the magnetic intensity was controlled by altering the voltage of Potentiostatic Apparatus which was demarcated by Gauss Meter in advance. 2D IR correlation spectra were obtained by treatment of the series of dynamic spectra with 2D correlation analysis of FTIR software provided by Tsinghua University. The solid-state fluorescent spectra were recorded on an Edinburgh Instrument FL/FS-920 fluorescent spectrometer using Xe lamp for steady fluorescence and H_2 nanosecond flash lamp for transient fluorescence.

2.2. Synthesis of compounds

$\{[Pb_3(CPIDA)_2(H_2O)_3]\cdot H_2O\}_n$ **1**. A mixture of $Pb(NO_3)_2$ (0.066 g, 0.2 mmol) and H_3CPIDA (0.05 g, 0.2 mmol) was dissolved in *N*, *N*-dimethylform amide (DMF) and H_2O (1:1, 8 mL). The pH value was adjusted to 3.0 with HNO_3 (1.0 mol/L) and KOH (1.0 mol/L). The mixture was sealed in a 15 cm^3 teflon-lined stainless autoclave and heated at 90 °C for 3 d under autogenous pressure and then cooled to room temperature. Colorless block crystals were obtained in a yield of 78% (based on Pb). Anal. Calc for $C_{22}H_{24}Pb_3N_2O_{16}$: C, 22.13; H, 2.02; N, 2.35 wt%; Found: C, 22.20; H, 1.93; N, 2.42 wt%. IR (KBr, cm^{-1}): 3199 (w), 1601 (s), 1575 (vs), 1533 (s), 1394 (vs), 1306 (s), 1202 (w), 782 (m), 698(w), 652 (w).

$\{[Cd_3(CPIDA)_2(H_2O)_4]\cdot 5H_2O\}_n$ **2**. The synthesis method of **2** was similar to that of **1**, adding $Cd(NO_3)_2\cdot 4H_2O$ (0.062 g, 0.2 mmol) instead of $Pb(NO_3)_2$. The pH value was adjusted to 3.0 with HNO_3 (1.0 mol/L) and KOH (1.0 mol/L). Light yellow block crystals were obtained in a yield of 83% (based on Cd). Anal. Calc for $C_{22}H_{34}Cd_3N_2O_{21}$: C, 26.43; H, 3.43; N, 2.80 wt%; Found: C, 26.30; H, 3.37; N, 2.86 wt%. IR (KBr, cm^{-1}): 3354 (m), 1656 (m), 1590 (vs), 1403 (vs), 1306 (s), 1202 (m), 781 (m), 721 (w), 701(w), 647 (m).

$[Cd(HCPIDA)(bpy)(H_2O)]_n$ **3**. A mixture of $Cd(NO_3)_2\cdot 4H_2O$ (0.062 g, 0.2 mmol), H_3CPIDA (0.05 g, 0.2 mmol) and bpy (0.04 g, 0.25 mmol) was dissolved in DMF and H_2O solution (1:1, 8 mL). The pH value was adjusted to 2.2 with HNO_3 (1.0 mol/L) and KOH (1.0 mol/L). The mixture was sealed in a 15 cm^3 teflon-lined stainless autoclave and heated at 90 °C for 4 d under autogenous pressure and then cooled to room temperature. Colorless prism crystals were obtained in a yield of 56% (based on Cd). Anal. Calc for $C_{21}H_{19}CdN_3O_7$: C, 46.90; H, 3.56; N, 7.81 wt%; Found: C, 46.95; H, 3.42; N, 7.74 wt%. IR (KBr, cm^{-1}): 3446 (w), 2909 (vw), 1678 (m), 1603 (vs), 1412 (m), 1392 (m), 1303 (m), 1242 (m), 1191(m), 816 (w), 627 (w).

$\{[Co_3(CPIDA)_2(bpy)_3(H_2O)_4]\cdot 2H_2O\}_n$ **4**. The synthesis method of **4** was similar to that of **3**, adding $Co(NO_3)_2\cdot 6H_2O$ (0.058 g, 0.2 mmol) instead of $Cd(NO_3)_2\cdot 4H_2O$. The pH value was adjusted to 2.5 with HNO_3 (1.0 mol/L) and KOH (1.0 mol/L). Red prism crystals were obtained in a yield of 71% (based on Co). Anal. Calc for $C_{52}H_{52}Co_3N_8O_{18}$: C, 49.81; H, 4.18; N, 8.94 wt%; Found: C, 49.73; H, 4.24; N, 8.89 wt%. IR (KBr, cm^{-1}): 3398 (m), 2913 (m), 1586(vs), 1534(s), 1412 (s), 1380 (s), 1331(s), 1299 (s), 1247 (m), 1191 (m), 1068 (w), 813(m), 785 (w), 635 (m).

2.3. X-ray crystallography

The X-ray intensity data were collected at 293(2) K on a Bruker SMART APEX II X-ray diffractometer system with graphite-monochromated Mo$K\alpha$ radiation ($\lambda = 0.71073$ Å), using the φ and ω-scan technique. Absorption corrections were applied with SADABS. The structures were solved by the direct methods and successive Fourier difference syntheses, and refined by the full-matrix least-squares method on F^2 with anisotropic displacement parameters for all non-hydrogen atoms. The remaining hydrogen atoms were generated geometrically and not refined. The isotropic displacement parameters of all hydrogen atoms were defined as $U_{iso}(H) = 1.2U_{eq}(C)$. Further details of the crystallographic data and structure refinement for four compounds are tabulated in Table 1. Selected bond lengths and angels are listed in Tables 2–5. The corresponding parameters of hydrogen bonding in **2** and **4** are listed in Table 6. All calculations were performed on a computer with SHELXTL-PC program package [32,33].

3. Results and discussion

3.1. Structural description and discussion

$\{[Pb_3(CPIDA)_2(H_2O)_3]\cdot H_2O\}_n$ **1**. The single crystal X-ray analysis reveals that the seven-coordinated Pb1 is linked to six oxygen atoms from three carboxylate groups with chelating and bridging

Table 1
Crystallographic data for compounds **1**, **2**, **3** and **4**.

Compounds	**1**	**2**	**3**	**4**
Empirical formula	$C_{22}H_{24}Pb_3N_2O_{16}$	$C_{22}H_{34}Cd_3N_2O_{21}$	$C_{21}H_{19}CdN_3O_7$	$C_{26}H_{26}Co_{1.5}N_4O_9$
Formula mass	1194.00	999.71	537.79	626.90
Crystal system	Triclinic	Triclinic	Monoclinic	Monoclinic
Space group	*P*−1	*P*−1	$P2_1/c$	$P2_1/c$
a (Å)	10.601(2)	10.585(5)	21.460(4)	11.338(2)
b (Å)	11.773(2)	12.066(5)	10.300(2)	27.049(5)
c (Å)	12.609(3)	13.480(4)	9.2633(19)	8.7365(17)
α (°)	65.10(3)	95.530(17)	90	90
β (°)	82.81(3)	104.492(16)	90.50(3)	109.26(3)
γ (°)	74.17(3)	103.006(18)	90	90
V (Å^3)	1373.2(5)	1602.7(11)	2047.4(7)	2529.2(9)
Dc (g/cm^3)	2.888	2.072	1.745	1.646
Z	2	2	4	4
F(000)	1088	984	1072	1290
λ(Mo*Kα*) (Å)	0.71073	0.71073	0.71073	0.71073
Limiting indices	$-13\leqslant h\leqslant 13$; $-14\leqslant k\leqslant 13$; $-16\leqslant l\leqslant 16$	$-13\leqslant h\leqslant 13$; $-15\leqslant k\leqslant 15$; $-17\leqslant l\leqslant 16$	$-27\leqslant h\leqslant 27$; $-13\leqslant k\leqslant 13$; $-12\leqslant l\leqslant 9$	$-14\leqslant h\leqslant 14$; $-35\leqslant k\leqslant 31$; $-11\leqslant l\leqslant 10$
Goodness-of-fit on F^2	1.046	1.022	1.026	1.072
Collected reflections	10379	16016	15910	20301
Independent reflections(R_{int})	5911(0.0505)	7293(0.0335)	4677(0.0293)	5593(0.0555)
Observed reflections ($I>2\sigma(I)$)	5610	6509	4541	5009
Final *R* factors ($I>2\sigma(I)$)	R_1[a] = 0.0718	$R_1 = 0.0307$	$R_1 = 0.0306$	$R_1 = 0.0812$
	wR_2[b] = 0.1884	*wR*$_2$ = *0.0910*	*wR*$_2$ = *0.0806*	*wR*$_2$ = *0.2467*
Final *R* factors (all data)	$R_1 = 0.0740$	$R_1 = 0.0377$	$R_1 = 0.0325$	$R_1 = 0.0918$
	$wR_2 = 0.1920$	*wR*$_2$ = *0.0961*	*wR*$_2$ = *0.0821*	*wR*$_2$ = *0.2560*
Largest diff. map peak and hole eÅ^{-3}	7.322 and −5.890	0.877 and −1.598	0.521 and −0.486	0.647 and −0.686

[a] $R_1 = \sum||F_0|-|F_c||/\sum|F_0|$.
[b] $wR_2 = \{\sum[w(F_0^2-F_c)^2]/\sum[w(F_0^2)^2]\}^{1/2}$.

Table 2
Selected bond lengths (Å) and angles (°) for **1**.[a]

Pb(1)–O(2)#1	2.426(8)	Pb(1)–O(1)#1	2.459(8)
Pb(1)–O(4)	2.516(9)	Pb(1)–O(10)	2.644(8)
Pb(1)–O(3)	2.732(10)	Pb(1)–O(14)	2.815(12)
Pb(2)–O(8)	2.464(8)	Pb(2)–O(13)	2.382(10)
Pb(2)–O(6)	2.502(8)	Pb(2)–O(10)	2.465(8)
Pb(3)–O(12)#2	2.527(9)	Pb(2)–O(3)	2.609(9)
Pb(3)–O(11)#2	2.583(9)	Pb(3)–O(9)#3	2.561(8)
Pb(3)–O(5)	2.621(9)	Pb(3)–O(6)	2.614(8)
Pb(3)–O(15)#4	2.834(12)	Pb(3)–O(8)	2.690(8)
O(1)#1–Pb(1)–O(4)	81.4(3)	O(2)#1–Pb(1)–O(1)#1	53.1(3)
O(1)#1–Pb(1)–O(10)	124.7(3)	O(2)#1–Pb(1)–O(4)	77.1(3)
O(2)#1–Pb(1)–O(3)	75.9(3)	O(2)#1–Pb(1)–O(10)	77.9(3)
O(4)–Pb(1)–O(3)	49.0(3)	O(4)–Pb(1)–O(10)	113.9(3)
O(2)#1–Pb(1)–O(14)	120.3(3)	O(1)#1–Pb(1)–O(3)	116.2(3)
O(4)–Pb(1)–O(14)	63.7(3)	O(10)–Pb(1)–O(3)	65.8(3)
O(3)–Pb(1)–O(14)	104.9(3)	O(1)#1–Pb(1)–O(14)	77.0(3)
O(13)–Pb(2)–O(10)	77.0(3)	O(10)–Pb(1)–O(14)	158.3(3)
O(13)–Pb(2)–O(6)	87.2(3)	O(13)–Pb(2)–O(8)	78.2(3)
O(10)–Pb(2)–O(6)	152.7(3)	O(8)–Pb(2)–O(10)	124.4(3)
O(8)–Pb(2)–O(3)	154.7(3)	O(8)–Pb(2)–O(6)	72.4(3)
O(6)–Pb(2)–O(3)	86.9(3)	O(13)–Pb(2)–O(3)	86.6(4)
O(12)#2–Pb(3)–O(11)#2	50.0(3)	O(10)–Pb(2)–O(3)	70.3(3)
O(12)#2–Pb(3)–O(6)	125.1(3)	O(12)#2–Pb(3)–O(9)#3	74.9(3)
O(11)#2–Pb(3)–O(6)	80.7(3)	O(9)#3–Pb(3)–O(11)#2	117.5(3)
O(9)#3–Pb(3)–O(5)	75.3(3)	O(9)#3–Pb(3)–O(6)	119.8(3)
O(6)–Pb(3)–O(5)	50.3(2)	O(12)#2–Pb(3)–O(5)	93.6(3)
O(9)#3–Pb(3)–O(8)	163.0(3)	O(11)#2–Pb(3)–O(5)	80.6(3)
O(6)–Pb(3)–O(8)	67.1(3)	O(12)#2–Pb(3)–O(8)	115.0(3)
O(12)#2–Pb(3)–O(15)#4	78.2(4)	O(11)#2–Pb(3)–O(8)	78.1(3)
O(11)#2–Pb(3)–O(15)#4	101.7(3)	O(5)–Pb(3)–O(8)	116.2(3)
O(5)–Pb(3)–O(15)#4	166.3(3)	O(9)#3–Pb(3)–O(15)#4	92.0(3)
O(8)–Pb(3)–O(15)#4	77.4(3)	O(6)–Pb(3)–O(15)#4	143.2(3)

[a] #1 −*x*+1, −*y*+1, −*z*+2; #2 −*x*, −*y*+3, −*z*+1; #3 *x*−1, *y*, *z*; #4 −*x*, −*y*+2, −*z*+2.

modes and one water molecule with a longer distance being 2.815(12) Å. Pb2 lies in a distorted pentagonal-dipyramidal environment with the axial angle being 175.95(8)°. The equatorial

Table 3
Selected bond lengths (Å) and angles (°) for **2**.[a]

Cd(1)–O(1)#1	2.242(2)	Cd(1)–O(5)	2.257(3)
Cd(1)–O(4)	2.308(3)	Cd(1)–O(13)	2.311(3)
Cd(1)–O(8)	2.346(3)	Cd(1)–O(16)#2	2.541(4)
Cd(1)–N(1)	2.648(3)	Cd(2)–O(11)#3	2.223(3)
Cd(2)–O(14)	2.271(3)	Cd(2)–O(8)	2.286(3)
Cd(2)–O(9)	2.300(3)	Cd(2)–O(15)	2.403(3)
Cd(2)–O(4)	2.433(3)	Cd(2)–N(2)	2.685(3)
Cd(3)–O(5)#4	2.241(3)	Cd(3)–O(12)#3	2.251(3)
Cd(3)–O(2)#5	2.251(3)	Cd(3)–O(9)	2.297(3)
Cd(3)–O(15)	2.302(3)	Cd(3)–O(16)	2.320(3)
O(1)#1–Cd(1)–O(4)	103.91(10)	O(1)#1–Cd(1)–O(13)	167.17(15)
O(1)#1–Cd(1)–O(5)	95.36(10)	O(4)–Cd(1)–O(13)	79.10(14)
O(5)–Cd(1)–O(4)	134.89(9)	O(5)–Cd(1)–O(8)	149.21(9)
O(5)–Cd(1)–O(13)	90.92(13)	O(13)–Cd(1)–O(8)	80.77(14)
O(1)#1–Cd(1)–O(8)	88.17(9)	O(5)–Cd(1)–O(16)#2	68.29(10)
O(4)–Cd(1)–O(8)	72.78(9)	O(13)–Cd(1)–O(16)#2	85.47(15)
O(1)#1–Cd(1)–O(16)#2	86.47(10)	O(1)#1–Cd(1)–N(1)	96.58(9)
O(4)–Cd(1)–O(16)#2	151.69(10)	O(4)–Cd(1)–N(1)	68.25(9)
O(8)–Cd(1)–O(16)#2	81.46(10)	O(8)–Cd(1)–N(1)	140.76(9)
O(5)–Cd(1)–N(1)	69.31(9)	O(11)#3–Cd(2)–O(14)	170.17(11)
O(13)–Cd(1)–N(1)	96.11(15)	O(14)–Cd(2)–O(8)	89.64(11)
O(16)#2–Cd(1)–N(1)	137.59(10)	O(14)–Cd(2)–O(9)	83.78(11)
O(11)#3–Cd(2)–O(8)	98.67(11)	O(11)#3–Cd(2)–O(15)	89.06(10)
O(11)#3–Cd(2)–O(9)	94.02(11)	O(8)–Cd(2)–O(15)	147.88(9)
O(8)–Cd(2)–O(9)	134.23(9)	O(11)#3–Cd(2)–O(4)	84.16(10)
O(14)–Cd(2)–O(15)	81.11(11)	O(8)–Cd(2)–O(4)	71.57(9)
O(9)–Cd(2)–O(15)	75.53(10)	O(15)–Cd(2)–O(4)	78.35(9)
O(14)–Cd(2)–O(4)	93.58(11)	O(14)–Cd(2)–N(2)	93.57(10)
O(9)–Cd(2)–O(4)	153.85(9)	O(9)–Cd(2)–N(2)	67.33(9)
O(11)#3–Cd(2)–N(2)	94.41(9)	O(4)–Cd(2)–N(2)	138.80(9)
O(8)–Cd(2)–N(2)	67.96(9)	O(5)#4–Cd(3)–O(2)#5	87.33(11)
O(15)–Cd(2)–N(2)	142.85(9)	O(5)#4–Cd(3)–O(9)	171.19(10)
O(5)#4–Cd(3)–O(12)#3	99.48(11)	O(2)#5–Cd(3)–O(9)	92.54(11)
O(12)#3–Cd(3)–O(2)#5	170.24(12)	O(12)#3–Cd(3)–O(15)	90.14(12)
O(12)#3–Cd(3)–O(9)	81.80(11)	O(9)–Cd(3)–O(15)	77.60(10)
O(5)#4–Cd(3)–O(15)	111.05(11)	O(12)#3–Cd(3)–O(16)	98.05(13)
O(2)#5–Cd(3)–O(15)	80.85(11)	O(9)–Cd(3)–O(16)	98.53(11)
O(5)#4–Cd(3)–O(16)	72.66(11)	O(2)#5–Cd(3)–O(16)	90.63(12)
O(15)–Cd(3)–O(16)	170.40(10)		

[a] #1 −*x*, −*y*+2, −*z*; #2 *x*−1, *y*, *z*; #3 −*x*+1, −*y*+1, −*z*+1; #4 *x*+1, *y*, *z*; #5 −*x*+1, −*y*+2, −*z*.

plane is defined by one nitrogen atom and four oxygen atoms from two separated iminodiacetate groups. However, Pb3 is eight-coordinated. Five oxygen atoms from the iminodiacetate groups present chelating bidentate and chelating/bridging bidentate modes; two oxygen atoms from the rigid carboxylate group adopt chelating mode; one water molecule also is involved with a longer distance Pb–O, 2.834(12) Å (Fig. 1). The bond lengths of Pb–O vary from 2.382(10) to 2.930(7) Å and the bond length of Pb–N is 2.835(0) Å, which are comparable to those reported in similar Pb(II) compounds [34–36].

Table 4
Selected bond lengths (Å) and angles (°) for **3**.[a]

Cd(1)–O(7)	2.259(2)	Cd(1)–O(4)	2.3027(18)
Cd(1)–O(1)#1	2.350(2)	Cd(1)–N(2)	2.376(2)
Cd(1)–O(1)#2	2.443(2)	Cd(1)–O(3)#3	2.4578(18)
Cd(1)–O(2)#2	2.526(2)	O(5)–C(11)	1.213(4)
O(6)–C(11)	1.326(4)	O(7)–Cd(1)–O(1)#1	83.26(8)
O(7)–Cd(1)–O(4)	155.19(7)	O(7)–Cd(1)–N(2)	106.30(10)
O(4)–Cd(1)–O(1)#1	83.41(7)	O(1)#1–Cd(1)–N(2)	164.34(8)
O(4)–Cd(1)–N(2)	83.04(9)	O(4)–Cd(1)–O(1)#2	86.31(7)
O(7)–Cd(1)–O(1)#2	109.18(7)	N(2)–Cd(1)–O(1)#2	114.87(7)
O(1)#1–Cd(1)–O(1)#2	71.98(7)	O(4)–Cd(1)–O(3)#3	77.66(6)
O(7)–Cd(1)–O(3)#3	80.89(6)	N(2)–Cd(1)–O(3)#3	82.19(7)
O(1)#1–Cd(1)–O(3)#3	87.26(7)	O(7)–Cd(1)–O(2)#2	82.29(7)
O(1)#2–Cd(1)–O(3)#3	155.15(6)	O(1)#1–Cd(1)–O(2)#2	112.52(7)
O(4)–Cd(1)–O(2)#2	122.24(6)	O(1)#2–Cd(1)–O(2)#2	52.42(6)
N(2)–Cd(1)–O(2)#2	81.52(7)	O(3)#3–Cd(1)–O(2)#2	152.21(7)

[a] #1 $-x+2, y-1/2, -z+3/2$; #2 $x, -y+3/2, z-1/2$; #3 $x, -y+1/2, z-1/2$.

Table 5
Selected bond lengths (Å) and angles (°) for **4**.[a]

Co(1)–O(8)	2.101(4)	Co(1)–O(8)#1	2.101(4)
Co(1)–O(6)	2.114(4)	Co(1)–O(6)#1	2.114(4)
Co(1)–N(4)	2.140(5)	Co(1)–N(4)#1	2.140(5)
Co(2)–O(7)	2.096(4)	Co(2)–O(4)	2.121(4)
Co(2)–N(1)	2.122(4)	Co(2)–O(3)#2	2.155(4)
Co(2)–N(2)#3	2.158(5)	Co(2)–O(5)	2.160(4)
O(8)–Co(1)–O(6)	93.03(15)	O(8)–Co(1)–O(6)#1	86.97(15)
O(8)–Co(1)–N(4)	91.68(18)	O(7)–Co(2)–O(4)	163.95(16)
O(6)–Co(1)–N(4)	91.37(17)	O(4)–Co(2)–N(1)	94.15(17)
O(8)–Co(1)–N(4)#1	88.32(18)	O(4)–Co(2)–O(3)#2	76.54(15)
O(6)–Co(1)–N(4)#1	88.63(17)	O(7)–Co(2)–N(2)#3	90.50(18)
O(7)–Co(2)–N(1)	90.76(18)	N(1)–Co(2)–N(2)#3	172.91(18)
O(7)–Co(2)–O(3)#2	88.23(16)	O(7)–Co(2)–O(5)	80.75(15)
N(1)–Co(2)–O(3)#2	89.74(16)	N(1)–Co(2)–O(5)	85.33(16)
O(4)–Co(2)–N(2)#3	86.50(18)	N(2)#3–Co(2)–O(5)	87.98(17)
O(3)#2–Co(2)–N(2)#3	97.27(17)	O(4)–Co(2)–O(5)	114.85(15)
O(3)#2–Co(2)–O(5)	167.85(15)		

[a] #1$-x+1, -y+1, -z$; #2 $x, -y+3/2, z-1/2$; #3 $x-1, y, z$.

The coordination modes of $CPIDA^{3-}$ in **1** are shown in Scheme 1(a) and (b). (a) The rigid carboxylate group cheats one Pb ion and the iminodiacetate group adopts chelating/bridging bis-bidentate modes with a big eight-member ring, leading to Pb clusters. (b) The rigid carboxylate group shows chelating bidentate. The iminodiacetate group with bridging bis-bidentate mode and the nitrogen atom connect Pb ions to generate two five-member rings $PbNC_2O$. In this way, the Pb clusters are connected by the flexible iminodiacetate groups to give 2D sheets on *ac* plane with the Pb···Pb distances ranging from 4.080(3) to 4.625(0) Å, which are further linked by $CPIDA^{3-}$ spacers in a head-to-tail mode to form a novel 3D porous framework. Because of the flexible and twisted iminodiacetate arms, there are three parallel channels along *a* axis: A, B, and C in the 3D framework (Fig. 2). Channels A are occupied by guest water molecules, whereas channels B and C are empty. The total void value of the channels without water guests is estimated to be 39.1 $Å^3$ by PLATON software, approximately 2.9% of the total crystal volume of 1373.2(5) $Å^3$.

$\{[Cd_3(CPIDA)_2(H_2O)_4]\cdot 5H_2O\}_n$ **2**. The single crystal X-ray analysis reveals that Cd1 are bonded by one nitrogen atom and four oxygen atoms from two separated $CPIDA^{3-}$ and two water molecules, resulting in a distorted pentagonal-dipyramidal geometry. Cd2 adopts the same geometry. The equatorial plane is also defined by one nitrogen and four oxygen atoms, belonging to two separated bridging iminodiacetate groups and one water molecule. The axial positions are occupied with angle of 170.17(11)°. Cd3 is octahedrally coordinated by six oxygen atoms from two iminodiacetate groups and two water molecules (Fig. 3). The Cd–O and Cd–N bond lengths are in the range of 2.223(3)–2.541(4) Å and 2.648(3)–2.685(3) Å, respectively, which are comparable to those reported in similar Cd(II) compounds [3,37].

The coordination mode of $CPIDA^{3-}$ in **2** is shown in Scheme 1(c). The rigid carboxylate group adopts a bidentate mode. The iminodiacetate group displaying bridging bis-unidentate modes and the nitrogen atom connect Cd ions to generate two five-member rings $CdNC_2O$. Cd clusters are connected by the iminodiacetate groups affording chains with the Cd···Cd distances ranging from 3.518 (6) to 3.777(9) Å, which are cross-linked by $CPIDA^{3-}$ spacers in a head-to-tail mode to generate a 2D layer, displaying a window with 10.585 Å × 5.734 Å (Fig. 4a). The presence of the flexible iminodiacetate arms of $CPIDA^{3-}$ is very

Table 6
Parameters for O–H···O hydrogen bonds in compound **2**[a] and **4**.[b]

Compounds	D–H···A	d (D–H) (Å)	d (H···A) (Å)	d (D···A) (Å)	<DHA (°)
2	O13–H13B···O(11B)	0.84(2)	2.30(3)	3.068(6)	151(6)
	O14–H14A···O(10B)	0.856(19)	1.98(3)	2.768(5)	152(5)
	O14–H14B···O(17B)	0.852(19)	1.79(2)	2.638(5)	171(5)
	O15–H15A···O18	0.838(18)	2.04(3)	2.803(12)	151(4)
	O15–H15B···O3	0.822(18)	1.82(3)	2.602(4)	158(5)
	O16–H16A···O10	0.888(19)	2.47(2)	3.350(5)	169(6)
	O17–H17A···O(1C)	0.877(19)	1.95(3)	2.796(4)	162(6)
	O17–H17B···O(7D)	0.873(19)	1.84(2)	2.710(4)	171(5)
	O18–H18A···O(18E)	0.85(2)	2.32(8)	3.08(2)	149(13)
4	O7–HB7···O(4A)	0.85(2)	2.21(4)	2.964(6)	149(6)
	O7–HB7···O(3B)	0.85(2)	2.37(5)	3.078(6)	141(6)
	O7–HW7···O(2C)	0.85(2)	1.83(3)	2.657(6)	162(7)
	O8–HB8···O5	0.84(2)	2.01(3)	2.813(6)	158(7)
	O8–HB8···O7	0.84(2)	2.50(6)	3.064(6)	125(6)
	O8–HW8···O(1C)	0.85(2)	1.85(2)	2.697(7)	173(6)
	O9–HB9···O(1D)	0.87(2)	1.84(7)	2.644(10)	153(12)

[a] A, $-x+1, -y+1, -z+1$; B, $-x+1, -y+1, -z$; C, $x+1, y-1, z$; D, $x+1, y, z$; E, $-x+1, -y+2, -z$.
[b] A, $x, -y+3/2, z-1/2$; B, $x, y, z-1$; C, $x-1, y, z-1$; D, $x-1, y, z$.

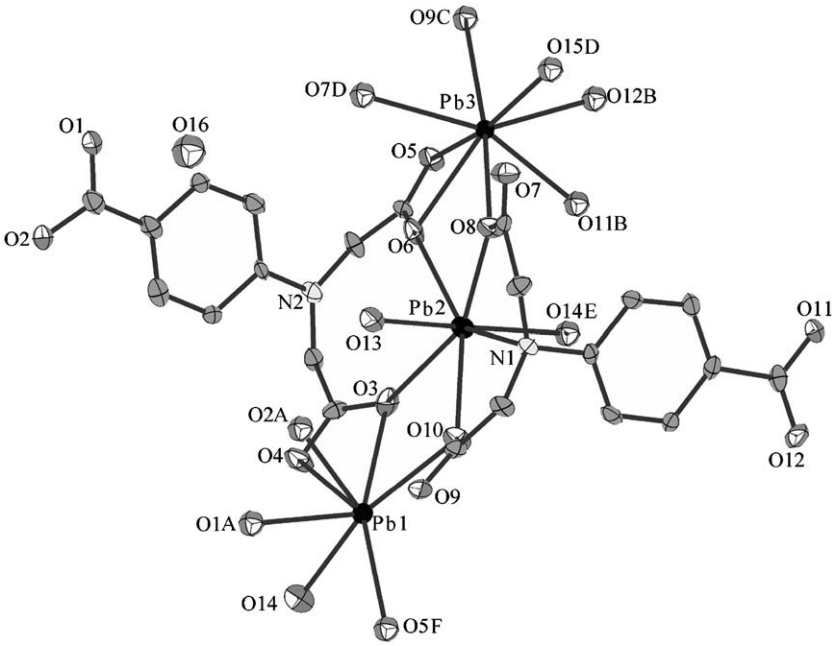

Fig. 1. The coordination environment of Pb(II) in **1** (40% thermal ellipsoids probability); all hydrogen atoms are omitted for clarity; symmetry codes: A, $-x+1$, $-y+1$, $-z+2$; B, $-x$, $-y+3$, $-z+1$; C, $x-1$, y, z; D, $-x$, $-y+2$, $-z+2$; E, $1-x$, $2-y$, $1-z$; F, $1+x$, y, z.

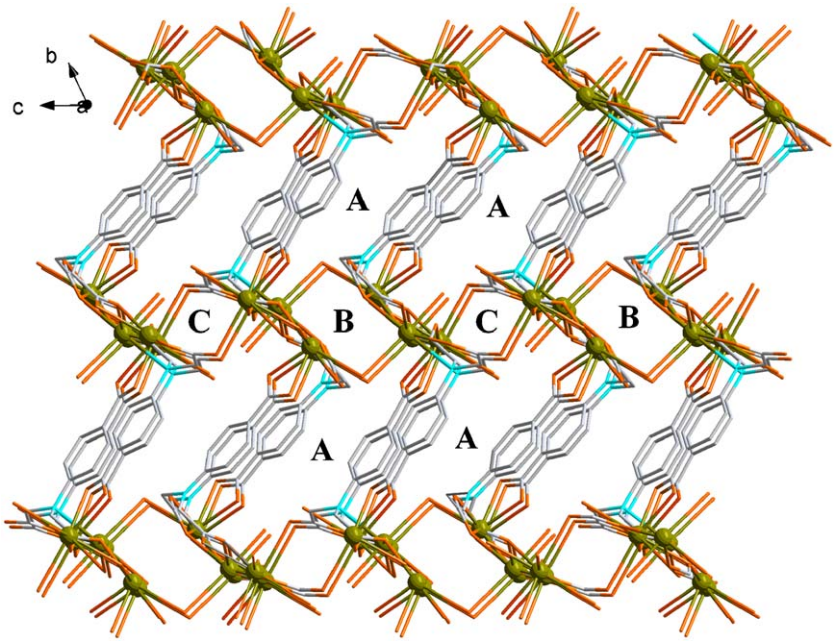

Fig. 2. Diagram of 3D porous framework architecture in **1**, guest water molecules and hydrogen atoms are omitted for clarity; color codes: Pb(II) (dark yellow), O (orange), N (blue), C (grey). (For interpretation of the references to color in this figure legend in, the reader is referred to the web version of this article.)

important for the formation of such a window. It is worth noting that the 2D layers have parallelogram-shaped channels with the dimension being 8.551 Å × 2.268 Å along *a* axis (Fig. 4b). Two guest water molecules occupied the channels, consolidated via the hydrogen bonding interactions (O18···O15, 2.803(12) Å; O18···O18E, 3.08(2) Å). Additionally, such 2D layers are further connected by strong hydrogen bonding interactions from water molecules and the carboxylate oxygen atoms (O14···O10B, 2.768(5) Å; O14···O17B, 2.638(5) Å; O16···O10, 3.350(5) Å; O17···O1C, 2.796(4) Å; O17···O7D, 2.710(4) Å) to form a 3D supramolecular framework (Table 6, Fig. 4b).

$[Cd(HCPIDA)(bpy)(H_2O)]_n$ **3**. The single crystal X-ray analysis indicates that Cd1 shows a distorted pentagonal-dipyramidal geometry with the equatorial plane consisting of one nitrogen atom from the bpy molecule and four oxygen atoms from the iminodiacetate groups. One iminodiacetate oxygen atom and the water molecule occupy the axial sites with the angle of 155.19(7)°. The bond lengths of Cd–O vary from 2.259(2) to 2.526(2) Å and the bond length of Cd–N is 2.376(2) Å, which are comparable to those reported in similar Cd(II) compounds [4,38,39].

The carboxylate groups are deprotonated partially in **3** supported by the presence of the characteristic band at

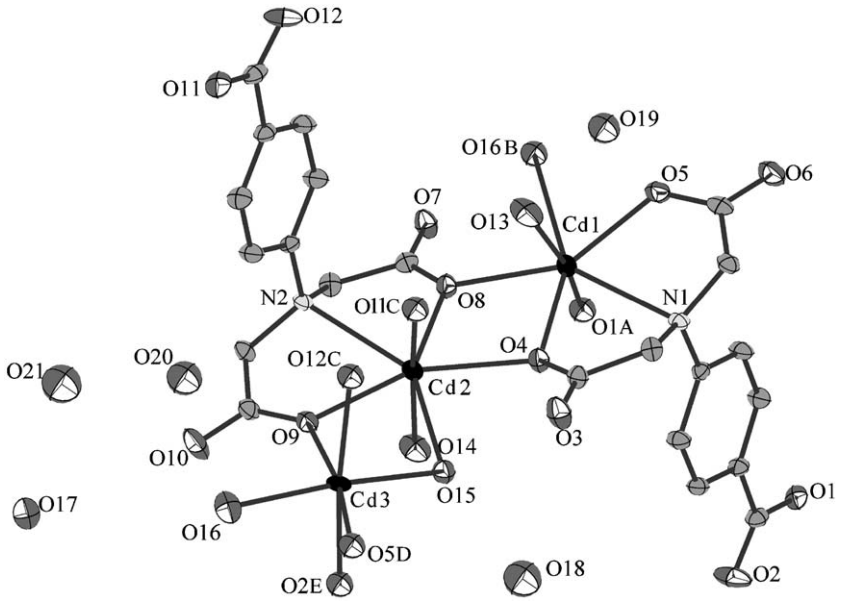

Fig. 3. The coordination environment around Cd(II) in **2** (40% thermal ellipsoids probability); all hydrogen atoms are omitted for clarity; symmetry codes: A, $-x$, $-y+2$, $-z$; B, $x-1$, y, z; C, $-x+1$, $-y+1$, $-z+1$; D, $x+1$, y, z; E, $-x+1$, $-y+2$, $-z$.

1678 cm^{-1} [40]. For the rigid carboxylate group remaining free, $HCPIDA^{2-}$ presents a new type of coordination mode as shown in Scheme 1(d). Two carboxylate groups of the iminodiacetate part exhibit different modes: one carboxylate group shows a bidentate mode and the other connects to two Cd ions in chelating/bridging bidentate modes. In **3**, the bpy liagnds adopt an unidentate mode with the dihedral angle between two pyridine rings being 46.60(0)°. So, it is very interesting that Cd ions are connected by the flexible iminodiacetate groups to give a 2D sheet on *bc* plane. The rigid aromatic rings of $HCPIDA^{2-}$ and the bpy ligands stand vertically along *a* axis above and below the 2D sheets (Fig. 5). In addition, these 2D sheets are stacked by weak π–π stacking interactions between pyridine rings of bpy molecules with the distances being centroid-to-centroid 4.343(6)Å, vertical face-to-face 3.821(2)Å and dihedral angle of 0.03(0)°.

$\{[Co_3(CPIDA)_2(bpy)_3(H_2O)_4]\cdot 2H_2O\}_n$ **4**. The single crystal X-ray analysis exhibits that there are two independent Co(II) sites and one of them (Co1) occupy the special site. So the asymmetric unit of **4** contains one and a half Co(II) ions, one $CPIDA^{3-}$ ligand, one and a half bpy molecules, two coordinated water molecules and one guest water molecule. Co1 displays a regular octahedral geometry, surrounded by four oxygen atoms from the iminodiacetate groups and water molecules in the equatorial plane. The nitrogen atoms from bpy molecules occupy the apical positions with the angle of 180.0(0)°. Whereas, the six-coordinated Co2 lies in a distorted octahedral geometry via coordinating to one water molecule, two nitrogen atoms from bpy molecules and three iminodiacetate oxygen atoms. The bond lengths of Co–O and Co–N are in the range of 2.096(4)–2.160(4)Å and 2.122(4)–2.158(5)Å, respectively, which are comparable to those reported in similar Co(II) compounds [41,42].

The coordination mode of $CPIDA^{3-}$ in **4** is shown in Scheme 1(e). The rigid carboxylate group does not participate in coordination and the flexible iminodiacetate group adopts bis-bidentate modes to connect Co atoms to form an eight-member ring. In that case, Co clusters are connected to afford a 2D sheet on *bc* plane. The rigid aromatic rings of $CPIDA^{3-}$ stand vertically above the 2D sheets. Whereas, the bpy molecules show a bridging bidentate mode with the dihedral angle between two pyridine rings being 41.03(4)°. So the adjacent sheets are pillared along *a* axis by bpy molecules to generate a novel 3D framework (Fig. 6a). The 3D framework is further consolidated by strong hydrogen bonding interactions between coordinated water molecules and the carboxylate oxygen atoms (O7⋯O2C, 2.657(6)Å; O7⋯O3B, 3.078(6)Å; O7⋯O4A, 2.964(6)Å; O7⋯O8, 3.064(6)Å; O8⋯O1C, 2.697(7)Å; O8⋯O5, 2.813(6)Å) (Table 6, Fig. 6b). On the other hand, one guest water is fixed to the framework through hydrogen bonding interaction (O9⋯O1D, 2.646(11)Å). In summary, the water molecules play important roles in the construction of the hydrogen bonds network. Additionally, there are offset π–π stacking interactions between aromatic rings from $CPIDA^{3-}$ ligands and pyridine rings of bpy molecules (centroid-to-centroid distance of 3.672(2)Å, vertical face-to-face distance of 3.388(8)Å and dihedral angle of 5.54(0)°).

3.2. Effect of synthetic conditions on the structures

As mentioned above, compounds **1**–**4** show various structures based on these five different coordination modes of H_3CPIDA in Scheme 1. 3D-framework **1** and 2D-layer **2** were obtained with Pb(II) and Cd(II) under the same conditions, respectively. Pb(II) ion has longer ionic radii than Cd(II), resulting in the higher coordination number and more flexible coordination geometry. The $CPIDA^{3-}$ ligands in **1** display two new types of coordination modes (chelating bidentate, chelating/bridging bis-bidentate and bridging bis-bidentate), which are more abundant than the simple bridging mode in **2**. In order to explore the potential coordination modes of $CPIDA^{3-}$ ligand, the auxiliary ligand bpy was introduced to **3** with Cd(II) ions. The $HCPIDA^{2-}$ ligands in **3** exhibit more charming chelating/bridging bidentate and bidentate modes in the presence of bpy molecules, without the five-member rings like what in **2**. But for the lower pH value in synthesis, the rigid carboxylate groups do not participate in coordination and the bpy molecules adopt the unidentate mode. Therefore, compound **3** still possesses a 2D sheet structure. As to **4**, the $CPIDA^{3-}$ ligands just show bis-bidentate with smaller ions Co(II), but the bpy ligands adopt bridging mode at a higher pH value. So compound **4** adopts a complicated 3D framework. Therefore, a rough conclusion could be made that selecting large metal ions and proper

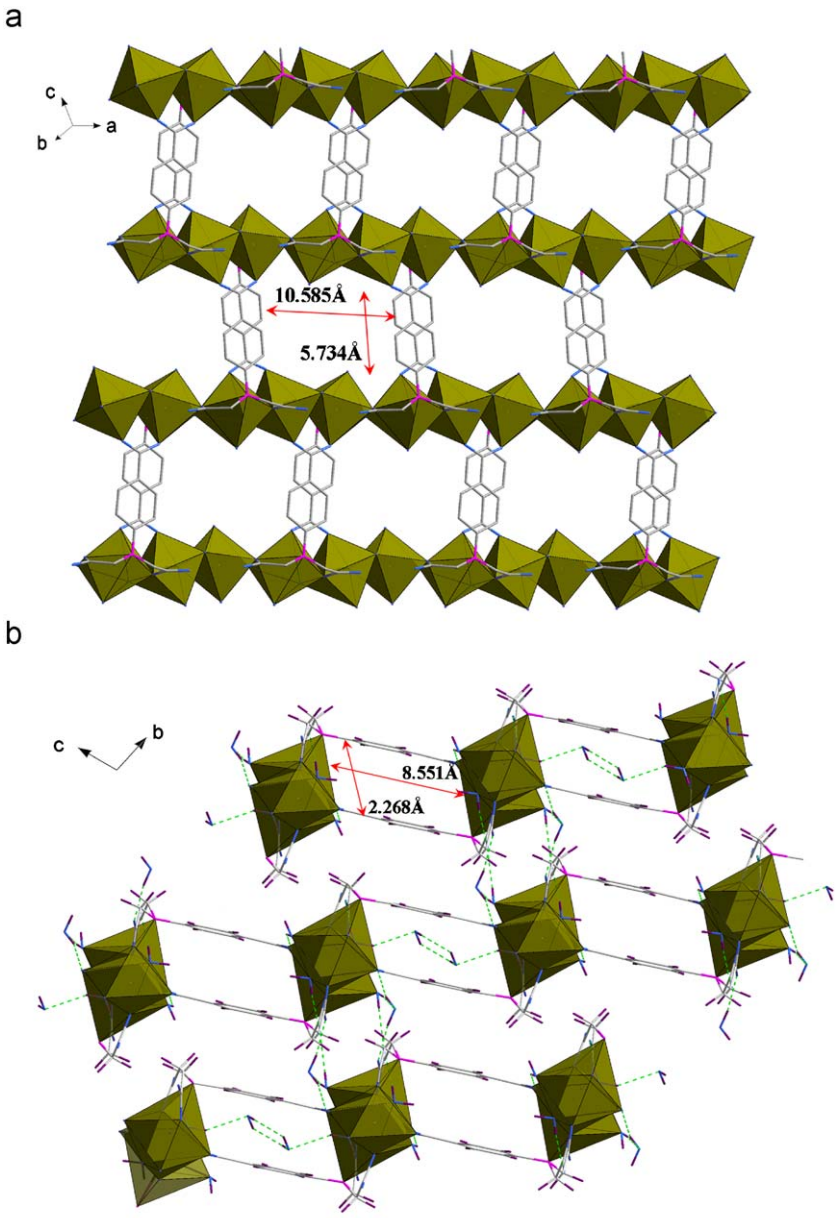

Fig. 4. (a) Polyhedron drawing of 2D layer architecture in **2**; guest water molecules and the hydrogen atoms are omitted for clarity; color codes: Cd (dark yellow polyhedron), O (blue), N (pink), C (grey). (b) 3D supramolecular framework of **2** stacked via hydrogen bonding interaction, green dashed lines represent hydrogen bonds; color codes: H (purple). (For interpretation of the references to color in this figure legend in, the reader is referred to the web version of this article.)

ligands and an increase of the pH value in the synthetic process would induce complication and higher dimensionality of the final structure to some extent, which is in agreement with the previous reports [43,44].

3.3. 2D correlation analysis of FTIR

In the FTIR spectrum of **4**, the board absorption at 3405 cm^{-1} is assigned to ν_{O-H} of water molecules. The characteristic bands overlapped in the range of 1650–1300 cm^{-1} are attributed to the anti-symmetric and symmetric stretching vibrations of the carboxylate groups $\nu_{C=O}$, benzene skeleton vibration, ν_{C-N}, ν_{C-C} and the bending vibrations of $-CH_2-$ in the flexible iminodiacetate groups of $CPIDA^{3-}$ [45,46]. In order to clarify the spectral features of the carboxylate groups in different modes, 2D correlation analysis of FTIR is applied in the spectral region of 1280–1630 cm^{-1} in **4**. Fig. 7 depicts the synchronous 2D correlation FTIR spectra of **4** with thermal and magnetic perturbation, respectively.

In Fig. 7(a), there are four strong autopeaks along the diagonal line at 1315, 1360, 1380 and 1585 cm^{-1} with thermal perturbation. The autopeaks at 1315 and 1360 cm^{-1} indicated the bending vibrations of $-CH_2-$ groups of the iminodiacetate groups are sensitive with thermal perturbation for the flexibility. Meanwhile, the autopeaks at 1380 and 1585 cm^{-1} from the symmetric and anti-symmetric $\nu_{C=O}$ explain that the stretching vibrations of COO on rigid carboxylate groups of $CPIDA^{3-}$ are sensitive with thermal perturbation. The absorption of uncoordinated carboxylate groups overlapped in 1D spectrum can be detected, via analyzing the 2D correlation FTIR spectra with thermal perturbation.

In Fig. 7(b), three strong autopeaks at 1333, 1375 and 1605 cm^{-1} along the diagonal line indicate that the symmetric and anti-symmetric $\nu_{C=O}$ of the coordinated carboxylate groups

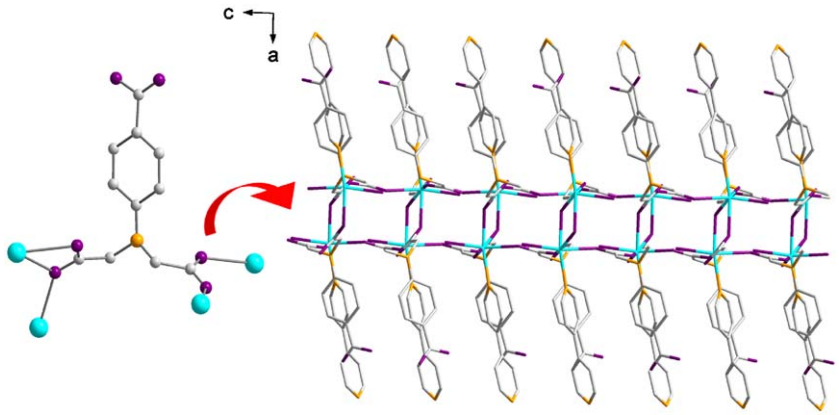

Fig. 5. 2D sheet structure in **3**, hydrogen atoms are omitted for clarity; showing the coordination mode of the ligand on the left side; color codes: Cd(II) (blue), O (purple), N (gold), C (grey). (For interpretation of the references to color in this figure legend in, the reader is referred to the web version of this article.)

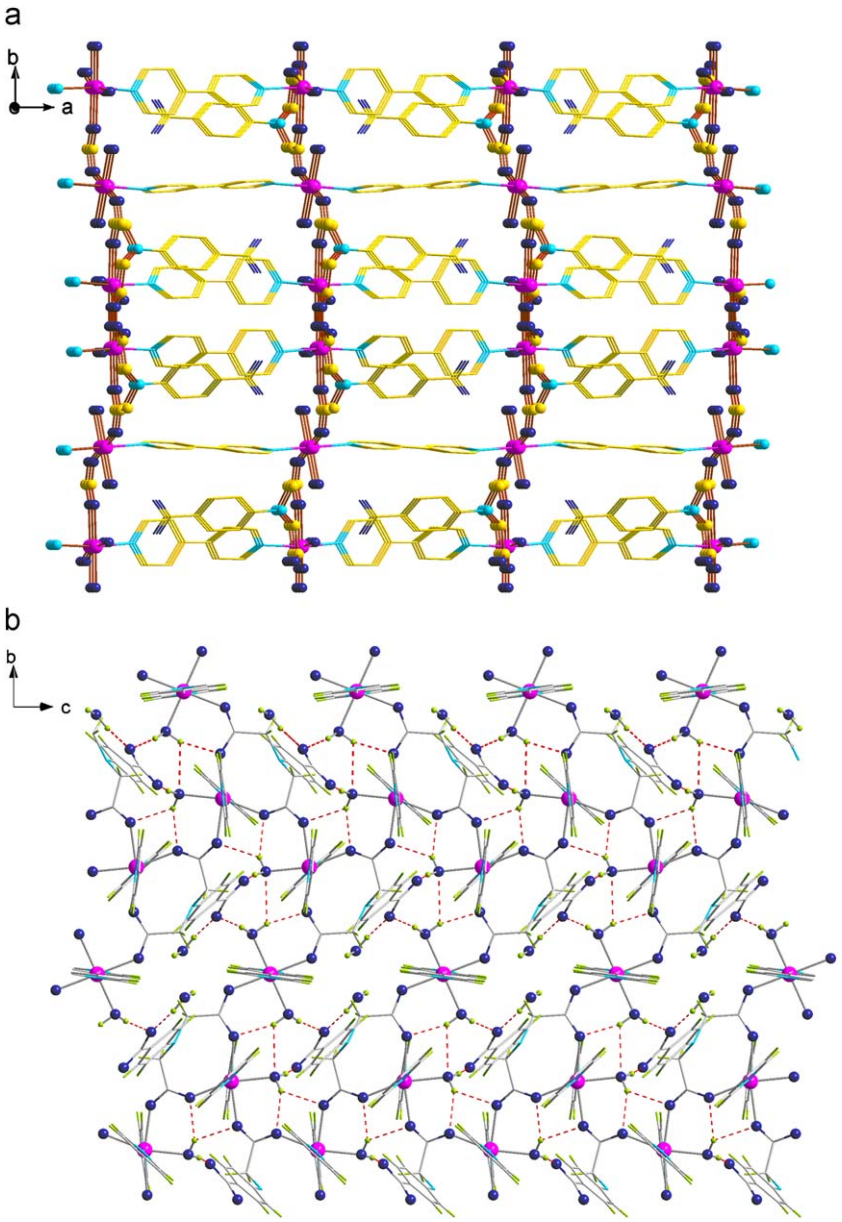

Fig. 6. (a) Diagram of 3D framework structure in **4**, guest water molecules and hydrogen atoms are omitted for clarity; color codes: Co(II) (pink), O (dark blue), N (blue), C (yellow). (b) View of hydrogen bonding interaction in 3D architecture of compound **4** along *a* axis, red dashed lines represent hydrogen bonds; Color codes: C (grey), H (green). (For interpretation of the references to color in this figure legend in, the reader is referred to the web version of this article.)

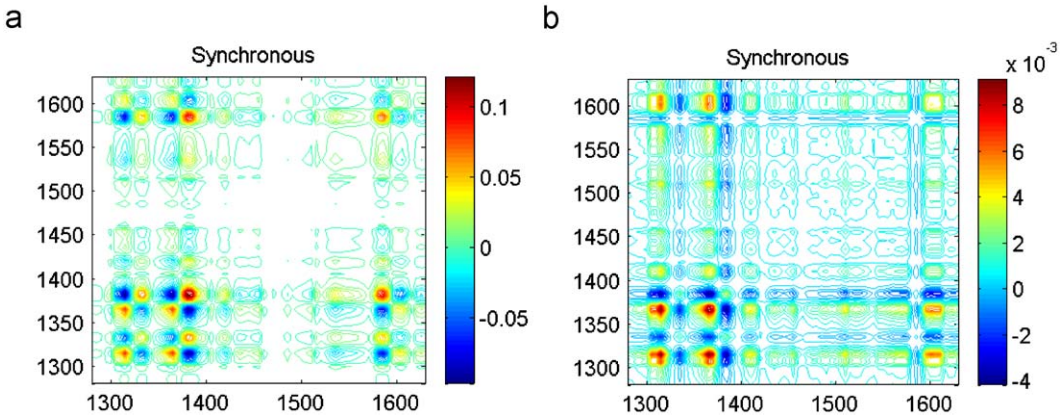

Fig. 7. The synchronous 2D correlation FTIR spectra of **4** in the range of 1280–1630 cm^{-1}: (a) with thermal perturbation; (b) with magnetic perturbation.

are very sensitive with magnetic perturbation. Moreover, two autopeaks at 1333 and 1375 cm^{-1} both from the symmetric $\nu_{C=O}$ indicate that there are two kinds of C=O lying in different magnetic environment, consistent with the coordination mode in **4**. Due to the interaction between magnetic particles and exoteric magnetic field, 2D correlation analysis of FTIR can probe the sensitive response of the groups coordinated to magnetic particles. So the absorption of different C=O of the coordinated carboxylate groups in **4** are detected in the 2D correlation FTIR spectra with magnetic perturbation [26].

3.4. Fluorescent properties

Compound **1** displays a strong shoulder emission at the range of 406 and 435 nm upon 340 nm excitation. Compound **2** exhibits an intense emission at 360 nm upon 335 nm excitation. Unfortunately, compound **3** is fluorescent silence, which maybe related with its 2D sheet structure. Excited at 310 nm, compound **4** exhibits an intense emission at the range of 380 and 400 nm and two weak emissions at 507 and 553 nm (Fig. 8). To further analyze the nature of these emission bands, the fluorescent property of H_3CPIDA has also been explored. The free H_3CPIDA molecule exhibits a weak peak at 356 nm and an intense peak at 433 nm upon 330 nm excitation. So the fluorescent peaks around 406 and 435 nm for **1** are contributed from the ligand-centered transitions (π–π^* and n–π^*) of $CPIDA^{3-}$ [47]. Because of the increase of conjugation upon metal coordination, the peaks have a red shift, compared with that of the free H_3CPIDA. With respect to **2,** the emission at 360 nm is attributed to the intraligand π–π^* transitions of $CPIDA^{3-}$ [16,18]. As for **4**, all the emission peaks belong to the ligand-centered transitions of $CPIDA^{3-}$ and the auxiliary bpy ligand. The emission bands were determined to be fluorescence based on the nanosecond-order decay lifetimes. Compound **1** exhibits a quenching of the fluorescence with $\tau_1 = 0.2666$ ns (96.38%) and $\tau_2 = 5.1817$ ns (3.62%). The lifetime for **2** is $\tau_1 = 2.504$ ns (20.66%) and $\tau_2 = 0.5286$ ns (79.34%).

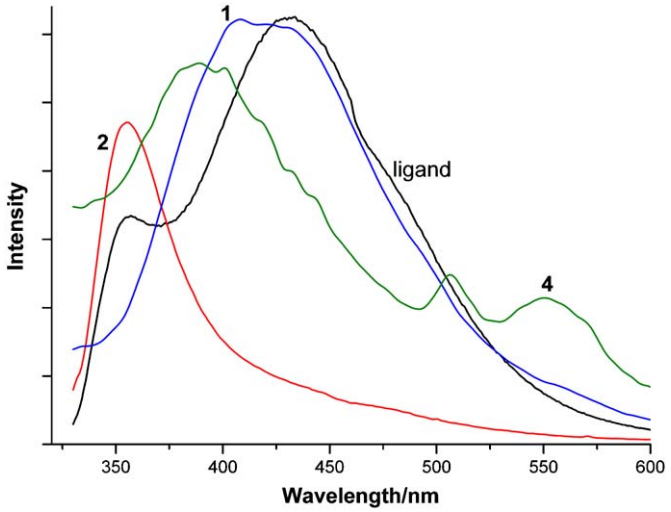

Fig. 8. Solid-state fluorescence emissions at room temperature for H_3CPIDA (black), compounds **1** (blue), **2** (red) and **4** (green). (For interpretation of the references to color in this figure legend in, the reader is referred to the web version of this article.)

4. Conclusions

In this research, four compounds with novel frameworks were successfully obtained from H_3CPIDA with divalent transition metal ions Pb(II), Cd(II) and Co(II) in the absence or presence of bpy ligands. The ligand H_3CPIDA exhibits five coordination modes for the strong coordinate abilities of the amino nitrogen and the carboxylate groups, based on the influence of the metal ions, the auxiliary bpy, the synthetic pH value, etc. Compounds **1** and **2** present 3D and 2D structure for the various coordination modes. On the other hand, compounds **3** and **4** show 2D and 3D framework basing on the different mode of bpy molecule. It is should be noted that employing 2D correlation analysis of FTIR, the characteristic bands of uncoordinated and coordinated carboxylate groups in **4** can be distinguished, depending on their different sensitivity to thermal and magnetic perturbation. So it is meaningful to explore more function of generalized 2D correlation FTIR spectroscopy with various perturbations, such as magnetism, light, heat, electricity, chemistry, etc. in MOFs. As a promising new type of multicarboxylate ligand, H_3CPIDA has a great potential in the field of coordination polymers. Further research on this system may focus on exploring more diverse coordination architectures of H_3CPIDA with other matel ions even lanthanide ions and the replacement of bpy with other bridge ligands to prepare novel polymeric compounds with higher dimensional structures and explore their valuable properties.

Supplementary data

Crystallographic data for the structures reported on this work have been deposited in the Cambridge Crystallographic Data Center with CCDC reference numbers 715032–715035 for **1**–**4**.

These data can be obtained free of charge at www.ccdc.cam.ac.uk/conts/retrieving.html [of from the Cambridge Crystallographic Data Center, 12, Union Road, Cambridge CB2 1EZ, UK; fax: (internat.) +441223 336-033; E-mail: deposit@ccdc.cam.ac.uk].

Acknowledgements

We gratefully acknowledge the financial support from National Nature Science Foundation of China (no. 20873021), the State Key Laboratory of Structure Chemistry, Fujian Institute of Research on the Structure of Matter, Chinese Academy of Sciences, and the Young Talent Programmed of Fujian Province (no. 2006F3072). We thank Prof. Sun Suqin (Tsinghua University, Beijing, China) for providing the 2D correlation FTIR analysis software.

Appendix A. Supplementary material

Supplementary data associated with this article can be found in the online version at doi:10.1016/j.jssc.2009.05.007.

References

[1] L. Carlucci, G. Ciani, D.M. Proserpio, Coord. Chem. Rev. 246 (2003) 247–289.
[2] Y. Su, S.Q. Zang, Y.Z. Li, H.Z. Zhu, Q.J. Meng, Cryst. Growth Des. 7 (2007) 1277–1283.
[3] L. Wang, M. Yang, G.H. Li, Z. Shi, S.H. Feng, Inorg. Chem. 45 (2006) 2474–2478.
[4] X. Shi, G.S. Zhu, X.H. Wang, G.H. Li, Q.R. Fang, X.J. Zhao, G. Wu, G. Tian, M. Xue, R.W. Wang, S.L. Qiu, Cryst. Growth Des. 5 (2005) 341–346.
[5] C.N.R. Rao, S. Natarajan, R. Vaidhyanathan, Angew. Chem. Int. Ed. 43 (2004) 1466–1496.
[6] B. Moulton, M.J. Zaworotko, Chem. Rev. 101 (2001) 1629–1658.
[7] K. Barthelet, J. Marrot, D. Riou, G. Ferey, Angew. Chem. Int. Ed. 41 (2002) 281–284.
[8] J.L.C. Rowsell, E.C. Spencer, J. Eckert, J.A.K. Howard, O.M. Yaghi, Science 309 (2005) 1350–1354.
[9] B. Wang, A.P. Cote, H. Furukawa, M. O'Keeffe, O.M. Yaghi, Nature 453 (2008) 207–211.
[10] R. Banerjee, A. Phan, B. Wang, C. Knobler, H. Furukawa, M. O'Keeffe, O.M. Yaghi, Science 319 (2008) 939–943.
[11] J. Kim, B.L. Chen, T.M. Reineke, H.L. Li, M. Eddaoudi, D.B. Moler, M. O'Keeffe, O.M. Yaghi, J. Am. Chem. Soc. 123 (2001) 8239–8247.
[12] N.W. Ockwig, O. Delgado-Friedrichs, M. O'Keeffe, O.M. Yaghi, Accounts Chem. Res. 38 (2005) 176–182.
[13] J.C. Dai, X.T. Wu, Z.Y. Fu, C.P. Cui, S.M. Hu, W.X. Du, L.M. Wu, H.H. Zhang, R.O. Sun, Inorg. Chem. 41 (2002) 1391–1396.
[14] Z.R. Pan, H.G. Zheng, T.W. Wang, Y. Song, Y.Z. Li, Z.J. Guo, S.R. Batten, Inorg. Chem. 47 (2008) 9528–9536.
[15] G.P. Yong, S. Qiao, Z.Y. Wang, Y. Cui, Inorg. Chim. Acta. 358 (2005) 3905–3913.
[16] Y.Q. Xu, D.Q. Yuan, B.L. Wu, F.L. Jiang, Y.F. Zhou, M.C. Hong, Inorg. Chem. Commun. 8 (2005) 651–655.
[17] Q. Chu, G.X. Liu, T.A. Okamura, Y.Q. Huang, W.Y. Sun, N. Ueyama, Polyhedron 27 (2008) 812–820.
[18] G.P. Yong, Z.Y. Wang, Y. Cui, Eur. J. Inorg. Chem. (2004) 4317–4323.
[19] G.P. Yong, Z.Y. Wang, J.T. Chen, J. Mol. Struct. 707 (2004) 223–229.
[20] X.L. Wang, Q. Chao, E.B. Wang, X. Lin, Z.M. Su, C.W. Hu, Angew. Chem. Int. Ed. 43 (2004) 5036–5040.
[21] I. Noda, Y. Ozaki, Two-Dimensional Correlation Spectroscopy: Applications in Vibrational and Optical Spectroscopy, Wiley Interscience, West Sussex, 2004.
[22] I. Noda, Appl. Spectrosc. 47 (1993) 1329–1336.
[23] I. Noda, Appl. Spectrosc. 54 (2000) 994–999.
[24] I. Noda, A.E. Dowrey, C. Marcott, G.M. Story, Y. Ozaki, Appl. Spectrosc. 54 (2000) 236a–248a.
[25] Y.P. Chen, H.H. Zhang, C.C. Huang, Y.N. Cao, R.Q. Sun, W.J. Guo, Spectrochim. Acta A Mol. Biomol. Spectrosc. 63 (2006) 536–540.
[26] S. Zhang, Y.N. Cao, H.H. Zhang, X.C. Chai, Y.P. Chen, J. Solid State Chem. 181 (2008) 399–405.
[27] Y.P. Chen, X.M. Shen, H.H. Zhang, C.C. Huang, Y.N. Cao, R.Q. Sun, Vib. Spectrosc. 40 (2006) 142–147.
[28] Y.P. Chen, H.H. Zhang, D.M. Ke, X.M. Shen, C.C. Huang, R.Q. Sun, Chin. J. Struct. Chem. 24 (2005) 1033–1038.
[29] Y.P. Chen, H.H. Zhang, X.Z. Wang, C.C. Huang, Y.N. Cao, R.Q. Sun, J. Solid State Chem. 179 (2005) 1674–1680.
[30] Y.N. Cao, H.H. Zhang, C.C. Huang, Q.Y. Yang, Y.P. Chen, R.Q. Sun, F.L. Zhang, W.J. Guo, J. Solid State Chem. 178 (2005) 3563–3570.
[31] Y.Q. Xu, D.Q. Yuan, B.L. Wu, L. Han, M.Y. Wu, F.L. Jiang, M.C. Hong, Cryst. Growth Des. 6 (2006) 1168–1174.
[32] G.M. Sheldrick, SHELXS-97, Program for X-ray Crystal Structure Solution, University of Gottingen, Gottingen, Germany, 1997.
[33] G.M. Sheldrick, SHELXL-97, Program for X-ray Crystal Structure Refinement, University of Gottingen, Gottingen, Germany, 1997.
[34] H.P. Xiao, A. Morsali, Solid State Sci. 9 (2007) 155–158.
[35] J. Sanchiz, P. Esparza, D. Villagra, S. Dominguez, A. Mederos, F. Brito, L. Araujo, A. Sanchez, J.M. Arrieta, Inorg. Chem. 41 (2002) 6048–6055.
[36] Q.F. Xu, Q.X. Zhou, J.M. Lu, X.W. Xia, Y. Zhang, J. Solid State Chem. 180 (2007) 207–212.
[37] M.A. Braverman, R.M. Supkowski, R.L. LaDuca, J. Solid State Chem. 180 (2007) 1852–1862.
[38] J. Tao, X.M. Chen, R.B. Huang, L.S. Zheng, J. Solid State Chem. 170 (2003) 130–134.
[39] Z.F. Tian, Y. Su, J.G. Lin, Q.J. Meng, Polyhedron 26 (2007) 2829–2836.
[40] L.J. Bellamy, The Infrared Spectra of Complex Molecules, Wiley, New York, 1958.
[41] Z.Y. Fu, X.T. Wu, J.C. Dai, S.M. Hu, W.X. Du, H.H. Zhang, R.Q. Sun, Eur. J. Inorg. Chem. (2002) 2730–2735.
[42] R.K. Chiang, N.T. Chuang, C.S. Wur, M.F. Chong, C.R. Lin, J. Solid State Chem. 166 (2002) 158–163.
[43] R.Q. Fang, X.M. Zhang, Inorg. Chem. 45 (2006) 4801–4810.
[44] Z.G. Guo, R. Cao, X.J. Li, D.Q. Yuan, W.H. Bi, X.D. Zhu, Y.F. Li, Eur. J. Inorg. Chem. (2007) 742–748.
[45] P. Koczon, J. Piekut, M. Borawska, W. Lewandowski, J. Mol. Struct. 651 (2003) 651–656.
[46] K. Nakamoto, 14a Infrared and Raman Spectra of Inorganic and Coordination Compounds, Wiley Interscience, New York, 1986.
[47] M. Du, X.J. Jiang, X.J. Zhao, Inorg. Chem. 46 (2007) 3984–3995.